Chin. Geogra. Sci. 2014 Vol. 24 No. 2 pp. 1–8
doi: 10.1007/s11769-014-0000-0

Springer Science Press
www.springerlink.com/content/1002-0063

A Neural Network Method for Monitoring Snowstorm: A Case Study in Southern China

MAO Kebiao[1, 2, 3], MA Ying[2, 3], XIA Lang[1, 2], SHEN Xinyi[4], SUN Zhiwen[5], HE Tianjue[3], ZHOU Guanhua[6]

(1. *National Hulunber Grassland Ecosystem Observation and Research Station, Institute of Agricultural Resources and Regional Planning, Chinese Academy of Agricultural Sciences, Beijing* 100081, *China*; 2. *Guangzhou Institute of Geography, Guangzhou* 510070, *China*; 3. *Department of Geography, University of Toronto, Toronto M5S3G3, Canada*; 4. *Hydrometeorology and Remote Sensing Laboratory, University of Oklahoma, Norman* 73072, *USA*; 5. *Institute No*. 503 *of China Academy of Space Technology, Beijing* 100081, *China*; 6. *School of Instrumentation Science and Opto-electronics Engineering, Beijing University of Aeronautics & Astronautics, Beijing* 100191, *China*)

Abstract: It has been observed that low temperature, rainfall, snowfall, frost have never occurred over the past 50 years in the southern China， and weather in this area is very complex, so the monitoring equipments are few. Optical and thermal infrared remote sensing is influenced much by clouds, so the passive microwave AMSR-E (Advanced Microwave Scanning Radiometer-Earth Observing System) data are the best choice to monitor and analyze the development of disaster. In order to improve estimation accuracy, the dynamic learning neural network was used to retrieve snow depth. The difference of brightness temperatures of $TB_{18.7V}$ and $TB_{36.5V}$, $TB_{18.7H}$ and $TB_{36.5H}$, $TB_{23.8V}$ and TB_{89V}, $TB_{23.8H}$ and TB_{89H} are made as four main input nodes and the snow depth is the only one output node of neural network. The mean and the standard deviation of retrieval errors are about 4.8 cm and 6.7 cm relative to the test data of ground measurements. The application analysis indicated that the neural network can be utilized to monitor the change of snow intensity distribution through passive microwave data in the complex weather of the southern China.
Keywords: snowstorm; neural network; snow depth; passive microwave; AMSR-E

Citation: Mao Kebiao, Ma Ying, Shen Xinyi, Xia Lang, Sun Zhiwen, He Tianjun, Zhou Guanhua. A neural network method for monitoring snowstorm: A case study in southern China . *Chinese Geographical Science*, doi: 10.1007/s11769-014-0000-0 2014 24(0): 000–000.

1 Introduction

Snow cover significantly influences the Earth′s surface energy balance and acts as the frozen storage in water balance. Snow parameters (especially snow water equivalent) are important variables for flood forecasting and the management of water resources, such as reservoir management and agricultural production activities (Jiang *et al*., 2007). Many experiments like Cold Land Processes, World Climate Research Programme, Climate and Cryosphere, Global Energy and Water Cycle Experiment have been made by many scientific research organizations, but people still do not have sufficient capacity to predict and assess the influence of snowstorm. Snow cover and snow water equivalent (SWE) data are usually monitored through traditional meteorological stations, which are poorly distributed globally in the point form (Robinson *et al*., 1993). However, the number of meteorological stations is often not enough and the distribution is not at random, especially for moun-

Received date: 2012-02-26; accepted date: 2013-07-29
Foundation item: Under the auspices of National Program on Key Basic Research Project (No. 2010CB951503), National Key Technology R & D Program of China (No. 2013BAC03B00), National High Technology Research and Development Program of China (No. 2012AA120905)
Corresponding author: MAO Kebiao. E-mail: maokebiao@126.com

tainous region.

The remote sensing technology provides a chance for us to quickly and efficiently obtain a large area of snow cover, snow depth, and many other parameters. It has been about 30 years to use remote sensing technology for monitoring snow. The methods to estimate the snow cover for visible and near infrared sensors, such as Moderate Resolution Imaging Spectroradiometer (MODIS) and National Oceanic and Atmospheric Administration/ Advanced Very High Resolution Radiometer (NOAA/ AVHRR), are increasingly mature, but the estimations of snow depth and snow water equivalent are still at the development stage (Chang *et al*., 1987; Tait, 1998; Kelly *et al*., 2003; Langlois *et al*., 2011; Durand and Liu, 2012). The brightness temperature of frequencies at 3–90 GHz is sensitive to snow crystal characteristics, snow density, and snow water equivalent (Pulliainen *et al*., 1999; Wiesmann and Mätzler, 1999; Macelloni *et al*., 2001; Tsang and Kong, 2001). The influence for each frequency is different under different conditions. For example, the emission from dry snow is mainly affected by underlying soil dielectric and roughness properties at lower frequencies. The emission is sensitive to snow water equivalent and snow particle size at higher frequencies because the volume scattering by snow particles becomes important (Mätzler, 1996). So Microwave remote sensing has been proved to be very effective in obtaining snow parameters, especially for snow depth and snow water equivalent (Foster *et al*., 1984; Shi and Dozier, 2000; Derksen *et al*., 2005; Foster *et al*., 2005; Macelloni *et al*., 2005; Pulliainen *et al*., 2006). In particular, passive microwave remote sensing has become an important data source of snow cover information because of all-weather imaging capabilities, rapid revisit time, and the ability to derive quantitative estimates of SWE (Derksen *et al*., 2000; Jiang *et al*., 2007; Langlois *et al*., 2011; Durand and Liu, 2012,). Many researches have been done by using passive microwave remote sensing to obtain snow parameters and have obtained large progress in often snowy areas (Foster *et al*., 1997; Pulliainen and Hallikainen, 2001; Kelly and Chang, 2003; Roy *et al*., 2004; Tedesco *et al*., 2004).

Although low temperature and snow disasters are common meteorological disasters during the Chinese winter, especially in the Qinghai-Tibet Plateau, northern Xinjiang, Inner Mongolia and Northeast China, they rarely occur in the southern China (Dong *et al*., 2001; Qin and Sun, 2006; Zhang *et al*., 2009). But in 2008, there were four consecutive high-intensity snowfalls for more than 20 days which significantly struck the transportation, communication and electricity transmission lines. It has never occurred over the past 50 years in the southern China and the weather is very complex in this area, but little research is done on low-temperatures and snow disasters in the southern China. Optical and thermal infrared remote sensing data (like MODIS) is influenced much by clouds, and the resolution of passive microwave is low but high coverage which is suitable for monitoring disasters with large areas, so the passive microwave AMSR-E (Advanced Microwave Scanning Radiometer-Earth Observing System) data are the best choice to monitor and analyze the development of the disaster. In oder to improve the monitoring accuracy for snowstorm under complex weather conditions, this paper makes a case study by using microwave remote sensing data in South China. .

2 Materials and Methods

2.1 Study area

The climate differs from region to region because of the extensive and complex topography in China (Dong *et al*. 2001). The Changjiang (Yangtze) River serves as China′s official dividing line between north and south, to some extent, it is also the dividing line of climate because the water vapor content from north and south usually meets here. The water vapor content in the southern China is higher than that in the northern China because of the influence of the Pacific and Indian Oceans. Clouds are very thick in the southern China, especially in Changjiang River Valley, which makes radiation of microwave in the region more complex and different from the other regions of China. The area of severest cloud coverage suffered from low-temperature, frost, heavy rainfall and snowfall in early 2008 are selected as the research region, which mainly involves Hunan, Hubei, Anhui, Guizhou, Guangxi, Guangdong, Jiangsu, Jiangxi, Shanghai, Chongqing, Zhejiang and Fujian (Mao *et al*., 2009). The range of study area is marked blue in Fig. 1.

2.2 Data and processing

AMSR-E is a passive microwave radiometer, which observes atmospheric, land, oceanic, and cryospheric pa-

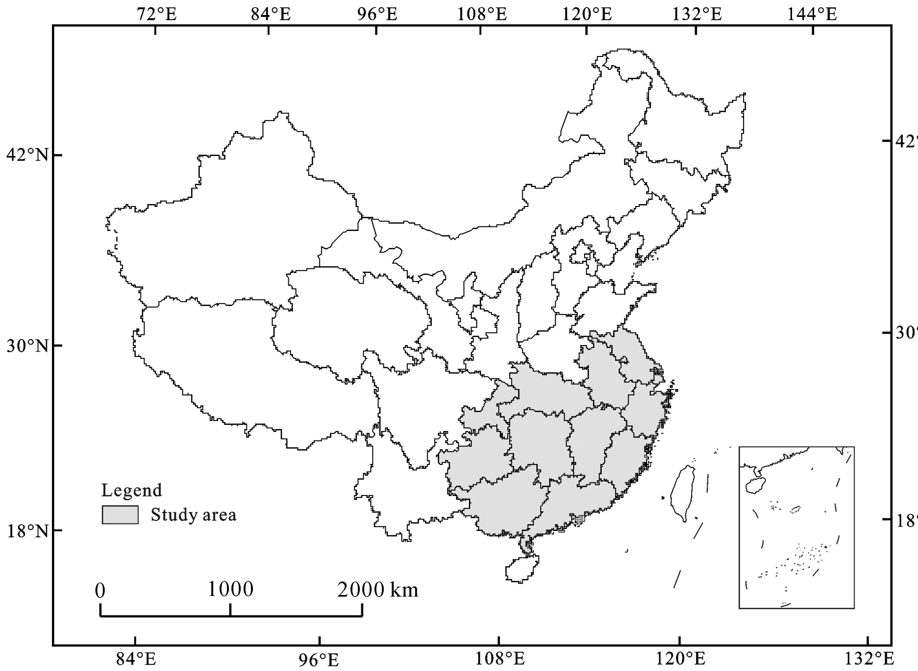

Fig. 1 Location of study area and distribution of part meteorological stations

rameters, including precipitation, sea surface temperature, ice concentration, snow water equivalent, surface wetness, wind speed, atmospheric cloud water, and water vapor content (Mao *et al.*, 2007a; 2007b). The AMSR-E Level 2A product (AE_L2A) contains brightness temperatures (TBs) at 6.9 GHz, 10.7 GHz, 18.7 GHz, 23.8 GHz, 36.5 GHz, and 89.0 GHz, which are resampled to be spatially consistent, and it is available at a variety of resolutions that correspond to the footprint sizes of the observations (56 km, 38 km, 24 km, 21 km, 12 km, and 5.4 km, respectively). The data can be downloaded freely from National Snow and Ice Data Center (http://nsidc.org/data/ae_l2a.html). In this study, the AMSR-E data with the resolution of 24 km × 24 km were used to monitor the change of snow area and the distribution of snow depth with the time. The brightness temperature can be obtained by Equation (1).

$$BT_i = Offset + DN \times Scale\_factor \qquad (1)$$

where BT_i is brightness temperature of frequency i; *Offset* and *Scale factor* can be obtained from the head file; *DN* is the value of the remote sensing image.

The study area has 818 meteorological stations covered in the southern China and parts of them are shown in Fig. 1. The ground measurement data in meteorological stations are collected to make comparisons and evaluations.

2.3 Neural Network

Neural networks learn from training data which need not be programmed to follow a specific mathematic equation. Many people (Tsang *et al.*, 1992; Tzeng *et al.*, 1994; Faure *et al.*, 2001; Tedesco *et al.*, 2004; Mao *et al.*, 2007b; 2008a; 2008b; 2010) used the neural networks to perform inversion for geophysical parameters and obtained good retrieval results. The dynamic learning neural network (DL) (Tzeng *et al.*, 1994) is selected to solve retrieval problems, which uses the Kalman filtering algorithm (Bletsas, 2005) to increase the convergence rate in the learning stage and enhance the separate ability for highly nonlinear boundaries problem. The initial neural network weights are set to be small random numbers (–1, 1). The Kalman filtering process is a recursive mean square estimation procedure. Each updated estimate of neural network weight is computed from the previous estimate and the new input data. The weights connected to each output node can be updated independently. The DL quickly achieves the required root mean square (rms) error in just a couple of iterations, and the result trained by NN is very stable. Thus the root error threshold is often set to be 0.001 and the epochs of iteration is two. More advantage of dynamic learning neural network than BP/FL (fasting learning) neural network can be found in reference (Tzeng *et al.*, 1994).

3 Results and Analyses

The AMSR-E data from January 10, 2008 to February 10, 2008 are downloaded from National Snow and Ice Data Center of US. One hundred and fourteen meteorological stations in the southern China are selected as ground data collection sites. A program has been made to read AMSR-E brightness temperatures from January 10, 2008 to February 10, 2008 by using the longitude and latitude as control condition. We collected 1524 data sets, and divided them randomly into two groups. The training data are 1101 sets and the testing data are 423 sets. The difference of brightness temperatures of $TB_{18.7V}$ and $TB_{36.5V}$, $TB_{18.7H}$ and $TB_{36.5H}$, $TB_{23.8V}$ and TB_{89V}, $TB_{23.8H}$ and TB_{89H} are made as four main input nodes and the snow depth is the only output node of neural network. After trial and error, we set the number of hidden-nodes from small to large, and selected the smallest of retrieval error for testing data (Table 1 is just part of data**)**. The mean and the standard deviation of retrieval error are about 4.8 cm and 6.7 cm relative to the ground measurement data when the number of the hidden layers is 2 and the number of hidden nodes is 350 in each layer.

Table 1 Summery of retrieval error

Hidden nodes	*R*	SD	Mean (cm)
50–50	0.65	8.5	6.8
100–100	0.66	8.3	6.6
150–150	0.68	8.2	6.4
200–200	0.71	7.8	6.1
250–250	0.73	7.2	5.4
300–300	0.75	6.9	5.1
350–350	0.78	6.7	4.8

Notes: R is correlation coefficient; SD is standard deviation of error

The neural network trained above was used to estimate the change of snow-depth from January 10th to February 10th 2008. The part of retrieval results is shown in Fig. 2, and the different color presents how much depth of snow. The disaster area reached maximum between January 28th and February 1st, 2008, which are consistent with the ground measurement. Figure 2c shows that the disaster is a very serious in Hunan, Guizhou, eastern of Sichuan, most part of Guangdong, Guangxi and Jiangxi provinces. The snow melted very quickly because weather changes were rapid in the southern China. A few values of estimation are anomalies with a big estimation error because the weather is

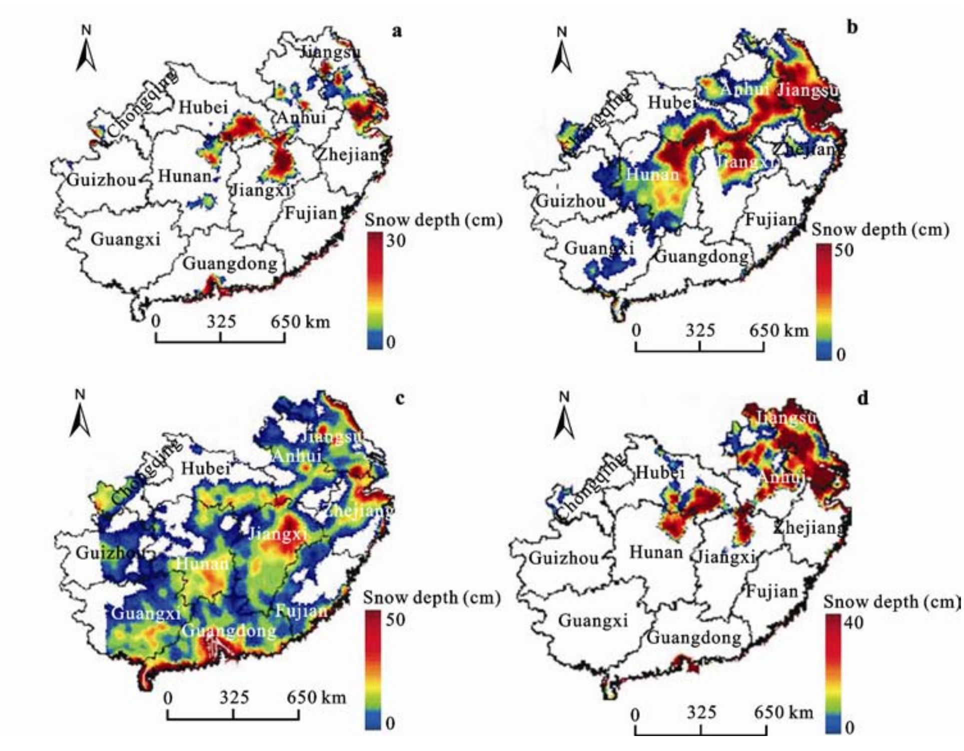

Fig. 2 Estimation of snow depth by neural networks in January 10, 2008 (a)**,** January 20, 2008 (b), January 30, 2008 (c), February 10, 2008 (d)

too complex in the southern China, so the scale of snow depth in Fig. 2 is adjusted according to the data from meteorological stations. Table 2 is part of disaster area information of the southern China obtained from meteorological stations.. Shown from Fig. 2 and Table 2, the disaster area estimated from AMSR-E data is consistent with the data obtained from ground meteorological stations.

Although the weather is very complex in the southern China, the snow is so large that the snow depth is relatively uniform in some places. Figure 3 is a comparison between estimation from AMSR-E data and ground measurement data from January 31, 2008 to February 10, 2008. The square of correlation coefficient is about 0.7, and the mean relative error is about 5.2 cm. Figure 2 indicates that the estimation error is large at the verge of sea and lake because the radiation mechanism is different between water surface and land surface. There are two main reasons (Mao *et al*., 2007a). The first is that there exists certain water like large lake in some AMSR-E pixels because the radioactive mechanism of water is different from others (soil and vegetation). The second is that there exists certain major rainfall in some AMSR-E pixels. On the other hand, the resolution of passive microwave data is very low, so there are many mixed pixels. In order to improve estimation accuracy, more research should be made further for mixed pixels covered by water and other influence factors, like topography, vegetation, mixed pixel.

Table 2 Disaster area in the southern China in 2008

Date	Disaster Area (km^2)	Date	Disaster area (km^2)
14, Jan.	321 800	1, Feb.	1 273 100
22, Jan.	400 500	3, Feb.	1 173 100
28, Jan.	1 164 100	5, Feb.	1 153 100
30, Jan.	1 313 100	7, Feb.	1 089 100

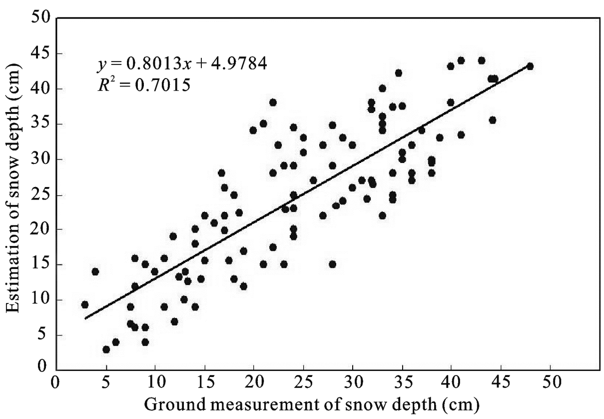

Fig. 3 Comparison of snow depth between estimation from AMSR-E data and ground measurement data

4 Discussion

It is very difficult for visible and thermal remote sensing to obtain ground information because there are much cloud and rainfall in the southern China, but microwave remote sensing can overcome this difficulty. The microwave radiometer measures the thermal emissions of the ground which transfer from the ground through the atmosphere to the remote sensor. According to the Raleigh-Jeans approximation for Planck function, the intensity of radiation observed by a radiometer can be simply written as Equation (2) (Mao *et al*., 2008c).

$$T_{\mathrm{bp}}(\tau,\mu)=(1-\omega)(1-e^{-\tau/\mu})T_{\mathrm{c}}+\varepsilon_{\mathrm{p}}T_{\mathrm{s}}e^{-\tau/\mu}+ t(1-t)(1-\varepsilon_{\mathrm{p}})T_{\mathrm{a}}^{\downarrow}+(1-t)T_{\mathrm{a}}^{\uparrow} \quad (2)$$

where p stands for horizontal (H) or vertical (V) polarization; $\mu=\cos\theta$; ε_{p} is emissivity; τ (equivalent canopy optical depth) and ω (the single scattering albedo) are two important parameters that characterize the absorbing and scattering properties of vegetation; T_{s} is land surface temperature; T_{c} is average temperature of vegetation; $T_{\mathrm{bp}}(\tau,\mu)$ is brightness temperature of radiation emitted by canopy at an angle θ; t is transmittance of atmosphere; $T_a^{\uparrow}$ is upwelling average atmosphere temperature; $T_{\mathrm{a}}^{\downarrow}$ is downwelling average atmosphere temperature. The centimeter wave band is influenced little by the atmosphere, and the transmittance (t) of microwave is very high and approximates to 1 even if the water vapor content is about 5 g/cm^2 in atmosphere (Ulaby *et al*., 1986), so the influence of atmosphere is very little and Equation (2) can be simplified to Equation (3).

$$T_{\mathrm{bp}}(\tau,\mu)=(1-\omega)(1-e^{-\tau/\mu})T_{\mathrm{c}}+\varepsilon_{\mathrm{p}}T_{\mathrm{s}}e^{-\tau/\mu} \quad (3)$$

T_{c} is usually assumed to be equal to T_{s} in soil covered by vegetation (Paloscia and Pampaloni, 1988; Njoku *et al*., 2003). τ (the canopy opacity) is function of vegetation water content (w), view angle (θ), and constant b (Njoku and Li, 1999) is like Equation (4).

$$\tau=\mathrm{b}w/\cos\theta \quad (4)$$

For bare soil, $\tau\approx 0$, thus the Equation (3) can be written as Equation (5).

$$T_{\mathrm{bp}}(\tau,\mu)=\varepsilon_{\mathrm{p}}T_s \quad (5)$$

For ground surface covered by snow, the emission of surface in the southern China is more complex than the description above. To determine the total emission from a snow layer above ground, the geometry of ground should be considered, which is shown in Fig. 4. The total emission source (T_{s}) within a layer can be separated into three components: the total upwelling emission (T_{us}), the total downwelling emission (T_{rds}), and the ground emission into the layer (T_{gs}). The ground emission is determined by the temperature and emissivity, which depends on the soil moisture and roughness of snow covered land. The emissivity is mainly influenced by dielectric constant which is a function of physical temperature, salinity, water content, soil texture and other factors (Dobson *et al*., 1985; Hallikainen and Jolma, 1986; Jiang *et al*., 2007). However, as shown by equations (2) to (5) and Fig. 4, the emission of ground surface is very complex. So it is very difficult to accurately estimate the snow depth from passive microwave remote sensing because a single frequency thermal measurement has at least two unknowns (emissivity and temperature) which is a typical ill-posed inversion problem. On the other hand, the dry snow emits considerably less microwave radiation than soil, and the brightness temperature of snow is inversely related to the snow water equivalent. When snow starts to melt, emission will significantly increase because water droplets absorb and re-emit rather than scatter microwave radiation (Foster *et al*., 2005; Jiang *et al*., 2007). So the retrieval is very complicated because different combination of snow, soil moisture, roughness, and land surface temperature may produce the same brightness temperature for single frequency. The relationship among emissivity, snow (*sw*), soil moisture (*sm*), roughness and temperature (T_{s}) can be depicted as Equation (6).

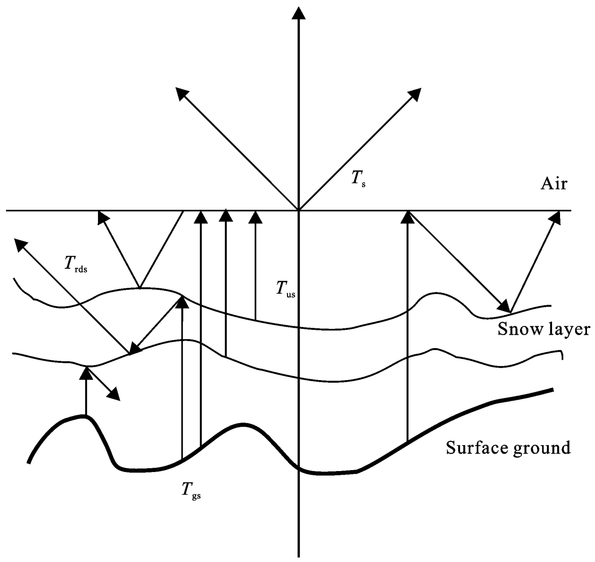

Fig. 4 Emission of ground surface covered snow

$$T_{\mathrm{s}} = f(T_{\mathrm{gs}}, T_{\mathrm{us}}, T_{\mathrm{rds}}, \varepsilon_{\mathrm{p}}, sw, sm, roughness) \quad (6)$$

The weather is very complex in the southern China. There are different types of cloud and rain in different regions. The rainfall, snowfall, snow and frost exist at the same time, and the status of snow changes with temperature. The different status of snow at different frequencies influences radiation of microwave differently. The emission of dry snow is considerably less than soil, so the brightness temperature of snow is inversely related to the snow water equivalent. When snow starts to melt, emission will significantly increase because water droplets absorb and re-emit rather than scatter microwave radiation (Foster *et al*., 2005; Jiang *et al*., 2007). The emission at lower frequencies from dry snow is mainly determined by the underlying soil dielectric and roughness properties. The emission at higher frequencies is more sensitive to snow water equivalent and snow particle size since the volume scattered by snow particles becomes important (Mätzler, 1996; Jiang *et al*., 2007). The general retrieval method is not very suitable for complex weather conditions (low-temperature, freezing, heavy rainfall and snowfall) of the southern China in early 2008. Another important reason is that most pixels are mixed-pixels for coarse spatial resolution of passive microwave (24 km × 24 km). The retrieval equations are so complex that a solution is often difficult to derive. Fortunately, the neural network is much different from conventional algorithm requiring that the inversion algorithm be known exactly. Neural network owns function approximation, optimization computation and classification ability which is composed of a large number of highly interconnected processing elements (neurons) working in parallel to solve a specific problem. All analysis indicates that neural network is more competent for retrieving snow depth in complex weather.

5 Conclusions

With the increasingly extreme climate changes, the monitoring of snowstorms in the southern China should be strengthened because the region has low levels of temperature, rainfall, snow, and frost at the same time. It is of urgent matter to monitor disasters via remote sensing images. Generally, for the geophysical parameters retrieval from passive microwave remote sensing data, it is very difficult to build a set of general retrieval equations due to many nonlinear and poorly understood factors. The analysis indicates that traditional methods can not depict all conditions well and is not suitable for the southern China.

In contrast to conventional methods, the neural network does not require that the relationship between input parameters and output parameters be known, since it is directly determined by the training data. Due to the fact that NN simultaneously owns function approximation, classification, optimization computation, and self-study ability, we can utilize neural network by using reliably measured ground data to estimate the snow depth. The mean and the standard deviation of retrieval errors are about 4.8 cm and 6.7 cm comparing with the test data of ground measurement data. The application analysis indicates that the neural network can be utilized to monitor changes in snow cover and the intensity distribution from passive microwave data. In order to improve estimation accuracy, more research should be made further for mixed pixels covered by water and other influence factors, such as topography, vegetation, mixed pixel.

Acknowledgments

The authors would like to thank the following people for their various help with this study: Chen Kunshan, Center for Space and Remote Sensing Research, National Central University. Tony, University of Toronto. We would also like to thank the anonymous reviewers and editors for their valuable comments, which greatly improved the presentation of this paper. Thanks to NASA providing AMSR-E/Aqua L2A Global Swath Spatially-Resampled Brightness Temperatures (Tb) V001 data, Boulder, CO, USA: National Snow and Ice Data Center.

References

Bletsas A, 2005. Evaluation of Kalman Filtering for Network Time Keeping, *IEEE Transactions on Ultrasonics, Ferroelectrics, and Frequency Control*, 52(9): 1452–1460. doi: 10.1109/TUFFC.2005.1516016

Chang A T C, Foster J L, Hall D K, 1987. NIMBUS-7 SMMR derived snow cover parameters. *Annals of Glaciology*, 9: 39–44.

Derksen C, LeDrew E, Walker A *et al*., 2000. Influence of sensor overpass time on passive microwave-derived snow cover parameters. *Remote Sensing of Environment*, 71(3): 297–308. doi: 10.1016/S0034-4257(99) 00084-X

Derksen C, Walker A, Goodison B *et al.*, 2005. Integrating in situ and multiscale passive microwave data for estimation of subgrid scale snow water equivalent distribution and variability. *IEEE Transactions on Geoscience and Remote Sensing*, 43(5): 960–972. doi: 10.1109/TGRS.2004.839591

Dobson M C, Ulaby F T, Hallikainen M T *et al.*, 1985. Microwave dielectric behavior of wet soil, part 2: Dielectric mixing models. *IEEE Transactions on Geoscience and Remote Sensing*, GE23(1): 35−46. doi: 0196-2892/84/0001-0035

Dong Wenjie, Wei Zhigang, Fan Lijun, 2001. Climatic character analyses of snow disasters in East Qinghai-Xizang Plateau livestock farm. *Plateau Meteorology*, 20(4): 402–406. (in Chinese)

Durand M, Liu D, 2012. The need for prior information in characterizing snow water equivalent from microwave brightness temperatures. *Remote Sensing of Environment*, 126 (12): 248–257. doi:10.1016/j.rse.2011.10.015

Faure T, Isaka H, Guillemet B, 2001. Neural network retrieval of cloud parameters of inhomogeneous and fractional clouds feasibility study. *Remote Sensing of Environment*, 77(2): 123–138. doi: 10.1016/S0034-4257(01)00199-7

Foster J L, Chang A T C, Hall D K, 1997. Comparison of snow mass estimates from prototype passive microwave snow algorithm, a revised algorithm and a snow depth climatology. *Remote Sensing of Environment*, 62(2): 132–142. doi: 10.1016/S0034-4257(97)00085-0

Foster J L, Hall D K, Chang A T C *et al.*, 1984. An overview of passive microwave snow research and results. *Reviews of Geophysics and Space Physics*, 22(2): 195–208.

Foster J L, Sun C, Walker J P *et al*., 2005. Quantifying the uncertainty in passive microwave snow water equivalent observations. *Remote Sensing of Environment*, 94(2): 187–203. doi: 10.1016/j.rse.2004.09.012

Hallikainen M T, Jolma P A, 1986. Retrieval of water equivalent of snow cover in Finland by satellite microwave radiometry. *IEEE Transactions on Geoscience and Remote Sensing*, GE24 (6): 855–862. doi: 0196-2892/86/1100-0855

Jiang L M, Shi J C, Tjuatja S *et al.*, 2007. A parameterized multiple-scattering model for microwave emission from dry snow. *Remote Sensing of Environment*, 111 (2–3): 357–366. doi: 10.1016/j.rse.2007.02.034

Kelly R E J, Chang A T C, 2003. Development of a passive microwave global snow depth retrieval algorithm for Special Sensor Microwave Imager (SSM/I) and Advanced Microwave Scanning Radiometer-EOS (AMSR-E) data. *Radio Science*, 38(4): 8076. doi: 10.1029 /2002RS002648

Kelly R J, Chang A T C, Tsang L *et al*. 2003. A prototype AMSR-E global snow area and snow depth algorithm. *IEEE Transactions on Geoscience and Remote Sensing*, 41(2): 1–13. doi: 10.1109/TGRS.2003.809118

Langlois A, Royer A, Dupont F *et al*., 2011. Improved corrections of forest effects on passive microwave satellite remote sensing of snow over boreal and subarctic regions. *IEEE Transaction on Geoscience and Remote Sensing*, 49(10): 3824–3837. doi: 10.1109/TGRS.2011.2138145

Macelloni G, Paloscia S, Pampaloni P *et al*., 2001. M., Microwave emission from dry snow: a comparison of experimental and model results. *IEEE Transactions on Geoscience and Remote Sensing*, 39(12): 2649–2656. doi: 0196-2892(01)09283-X

Macelloni G, Paloscia S, Pampaloni P *et al*., 2005. Monitoring of melting refreezing cycles of snow with microwave radiometers: The Microwave Alpine Snow Melting Experiment (MASMEx 2002–2003). *IEEE Transactions on Geoscience and Remote Sensing*, 43(11): 2431–2442. doi: 10.1109/TGRS.2005.855070

Mao K B, Li H T, Hu D Y *et al.* , 2010. Estimation of water vapor content in near-infrared bands around 1 μm from MODIS data by using RM–NN. *Optics Express,* 18(9): 9542–9554. doi: 10.1364/OE.18.009542

Mao K B, Shi J C, Li Z L *et al*., 2007a. A physics-based statistical algorithm for retrieving land surface temperature from AMSR-E passive microwave data. *Science in China* (*Series D*), 50(7): 1115–1120. doi: 10.1007/s11430-007-2053-x

Mao K B, Shi J C, Li Z L *et al*., 2007b. An RM-NN algorithm for retrieving land surface temperature and emissivity from EOS/ MODIS data, *Journal of Geophysical Research-Atmosphere*, 112, D21102: 1–17. doi: 10.1029/ 2007JD008428

Mao K B, Shi J C, Tang H J *et al*., 2008a. A neural network technique for separating and surface emissivity and temperature from ASTER imagery. *IEEE Transactions on Geoscience and Remote Sensing*, 46(1): 200–208.

Mao K B, Tang H J, Wang X F *et al.*, 2008b. Near-Surface air temperature estimation from ASTER data using neural network. *International Journal of Remote Sensing*, 29(20): 6021–6028. doi: 10.1080/01431160802192160

Mao K B, Tang H J, Zhang L X *et al*., 2008c. A Method for retrieving soil moisture in Tibet region by utilizing microwave index from TRMM/TMI Data. *International Journal of Remote Sensing*, 29(10): 2903–2923. doi: 10.1080/01431160701442104

Mao Kebiao, Tang Huajun, Zhou Qingbo *et al.*, 2009. Supervision and Analysis on Southern China's Snow Disaster in 2008 by Using Passive Microwave Data AMSR-E. *Chinese Journal of Agricultural Resources and Regional Planning*, 30(1): 46–50. (in Chinese)

Mätzler C, 1996. Microwave permittivity of dry snow. *IEEE Transactions on Geoscience and Remote Sensing*, 34(2): 573–581. doi: 0196-2892(96)01004

Njoku E G, Jackson T J, Lakshmi V *et al.*, 2003. Soil moisture retrieval from AMSR-E. *IEEE Transactions on Geoscience and Remote Sensing*, 41: 215–229. doi: 10.1109/TGRS.2002.808243

Njoku E G, Li L, 1999. Retrieval of land surface parameters using passive microwave measurements at 6–18 GHz. *IEEE Transactions on Geoscience and Remote Sensing*, 37(1): 79–93. doi: 0196-2892(99)00108-4

Paloscia S, Pampaloni P, 1988. Microwave polarization index for monitoring vegetation growth. *IEEE Transactions on Geoscience and Remote Sensing*, 26(5): 617–621. doi: 0196-2892/88/0900-0617

Pulliainen J T, Grandell J, Hallikainen M T, 1999. HUT snow emission model and its applicability to snow water equivalent retrieval. *IEEE Transactions on Geoscience and Remote Sensing*, 37(3): 1378–1390. doi: 0196-2892(99)03462-2

Pulliainen J, 2006. Mapping of snow water equivalent and snow depth in boreal and sub-arctic zones by assimilating space-borne microwave radiometer data and ground-based observations. *Remote Sensing of Environment*, 101: 257–269. doi: 10.1016/j.rse.2006.01.002

Pulliainen J, Hallikainen M, 2001. Retrieval of regional snow water equivalent from space-borne passive microwave observations. *Remote Sensing of Environment*, 75: 76–85. doi: S0034-4257(00)00157-7

Qin Zhengkun, Sun Zhaobo, 2006. Influence of abnormal East Asian winter monsoon on the northwestern Pacific sea temperature. *Chinese Journal of Atmospheric Sciences*, 30(2): 257–267. (in Chinese)

Robinson D A, Dewey K F, Heim R R, 1993. Global snow cover monitoring: an update. *Bulletin of the American Meteorological Society*, 74: 1689–1696.

Roy V, Goita K, Royer A *et al.*, 2004, Snow water equivalent retrieval in a Canadian boreal environment from microwave measurements using the HUT snow emission model. *IEEE Transactions on Geoscience and Remote Sensing*, 42(9): 1850–1859. doi: 10.1109/TGRS.2004.832245

Shi J, Dozier J, 2000. Estimation of Snow Water Equivalence Using SIR-C/X-SAR, Part I: Inferring snow density and subsurface properties. *IEEE Transactions on Geoscience and Remote Sensing*, 38(6): 2465–2474. doi: 0196-2892(00)07156-4

Tait A, 1998. Estimation of snow water equivalent using passive microwave radiation data. *Remote Sensing of Environment*, 64(3): 286–291. doi: 10.1016/S0034-4257(98)00005-4

Tedesco M, Pulliainen J, Takala M *et al*., 2004. Artificial neural network-based techniques for the retrieval of SWE and snow depth from SSM/I data. *Remote Sensing of Environment*, 90(1): 76–85. doi: 10.1016/j.rse.2003.12.002

Tsang L, Chen Z, Oh S *et al.*, 1992. Inversion of snow parameters from passive microwave remote sensing measurements by a neural network trained with a multiple scattering model. *IEEE Transactions on Geoscience and Remote Sensing*, 30(5): 1015–1024. doi: 019&2892/92

Tsang L, Kong J A, 2001. Scattering of electromagnetic waves. Advanced Topics. New York: Wiley-Interscience, 432.

Tzeng Y C, Chen K S, Kao W L *et al.*, 1994. A dynamic learning nerual network for remote sensing applications. *IEEE Transactions on Geoscience and Remote Sensing*, 32(5): 1096–1102. doi: 0196-289219

Ulaby F T, Moore R K, Fung A K, 1986. Microwave remote sensing: active Active and passive dedham. MA: Artech House, vol. 3. Dedham, Massachusetts.

Wiesmann A, Mätzler C, 1999. Microwave emission model of layered snowpacks. *Remote Sensing of Environment*, 70: 307–316. doi: 10.1016/S0034-4257(99)00046-2

Zhang Z, Gong D, Hu M *et al.*, 2009. Anomalous winter temperature and precipitation events in southern China. *Journal of Geographical Sciences*, 19: 471–488. doi: 10.1007/s11442-009-0471-8